Meteorology and Atmospheric Physics (2021) 133:41–54
https://doi.org/10.1007/s00703-020-00727-4

ORIGINAL PAPER

Spatiotemporal characteristics of drought in a semi-arid grassland over the past 56 years based on the Standardized Precipitation Index

Wei Li[1,2] · Limin Duan[2] · Wenjun Wang[1] · Yingjie Wu[1] · Tingxi Liu[2] · Qiang Quan[1] · Xiaojun Chen[1] · Hang Yin[1] · Quancheng Zhou[1]

Received: 9 July 2019 / Accepted: 14 January 2020 / Published online: 2 March 2020

Abstract
Drought is one of the major natural disasters in northern China. Therefore, monitoring and analyzing the changes of drought indices can provide scientific evidence for disaster assessment and for instituting policies for disaster prevention and mitigation. In this work, we used the gridded precipitation data set of a semi-arid steppe region in the Inner Mongolian Plateau from 1962 to 2017 to calculated the Standardized Precipitation Index (SPI) and the Standardized Precipitation Evapotranspiration Index (SPEI). By comparing the spatiotemporal distribution of the two indices with the historical drought records, we found that the SPI was more suitable for the drought description in the study area. Based on this, we calculate the SPI at different time scales (annual and seasonal), then depict the spatiotemporal variation of drought during the past 56 years by analyzing the frequency of drought events, drought frequency, and the station frequency ratio. The results indicate that in recent years, the degree of drought in the study area has increased, and the south-central regions are the highest occurrence area for different types of drought events. In addition, light drought occurs mostly in the autumn and is mainly distributed in the central and southern parts of the study area. The most extreme drought events often occur in the summer, and the highest frequency area is located in the western part of the study area. Large-scale light drought occurred in all seasons in the 1990s, while the domain moderate drought and the domain extreme drought occurred in the summers of 2001 and 2010, respectively.

1 Introduction

Global climate change leads to an imbalance between hydrothermal links in natural ecosystems. As a result, drought caused by moisture deficiencies has become increasingly frequent (IPCC 2013). In recent decades, with the continuous increase of drought intensity, frequency, range, and duration, this phenomenon has gradually become one of the most serious worldwide hydro-meteorological problems, with a significant impact on human society (Dai et al. 2004; Woodhouse and Overpeck 1998; Zuo et al. 2018). According to statistics and reports from the World Meteorological Organization (WMO), global meteorological disasters account for about 70% of all natural disasters, and drought disasters account for 50% of all meteorological disasters. Most regions in China are affected by the East Asian monsoon, and the country is seriously impacted by drought. According to statistics from the Ministry of Civil Affairs, in 2017 alone the area of agricultural crops affected by drought in China was over 9.8 million hectares, and 752.4 thousand hectares of that suffered from complete crop failure, causing direct economic losses of 37.5 billion Yuan.

With drought occurrence around the world becoming more severe day by day, the spatial and temporal distribution patterns of drought in China have also changed significantly in recent years (Dai 2011; Wang et al. 2014; Wen and Shen 2006). To describe the properties of drought development and to establish an efficient and scientific natural disaster prevention and treatment system, researchers in the field have conducted numerous analyses of drought characteristics, and the proposal and application

Responsible Editor: S. Fiedler.

Wei Li and Limin Duan contributed equally to this work.

✉ Tingxi Liu
txliu@imau.edu.cn

[1] Ministry of Water Resources of the People's Republic of China, Institute of Water Resource for Pastoral Area, Hohhot 010018, Inner Mongolia, China

[2] College of Water Conservancy and Civil Engineering/Inner Mongolia Water Resource Protection and Utilization Key Laboratory, Inner Mongolia Agricultural University, Hohhot 010018, Inner Mongolia, China

of drought indices have helped create a unified standard. The indices characterizing drought are usually classified into two categories: single-factor and multi-factor. The single-factor indices describe the drought change mainly through the key factor of precipitation, and such an index can better reflect the spatial and temporal characteristics of drought. Common indicators include the percentage of precipitation anomaly (Pa), the *Z*-Index and the Standard Precipitation Index (SPI).

A multi-factor index describes drought occurrence mainly from the perspective of the mechanisms of drought formation, which are primarily physical. However, such an index involves complicated calculations, and there is uncertainty in the data inputs, which can reduce the sensitivity of the index to some extent. Examples include the Palmer Drought Severity Index (PSDI), the Meteorological Drought Composite Index (CI), and the Standardized Precipitation Evapotranspiration Index (SPEI) (Vicente et al. 2010a, b; Wang et al. 2017; Yu et al. 2014a, b). Researchers worldwide have tested the applicability of various indices in combination with actual local drought conditions (Patel et al. 2007; Vicente et al. 2010a, b; Wu et al. 2007; Yu et al. 2014a, b; Zhang et al. 2013). Many argue that the application of a Standard Precipitation Index (SPI) can eliminate temporal and spatial differences in precipitation, making droughts comparable in time and space (Tao et al. 2014). Researchers have also proposed that such an index would have the advantages of obtaining parameters easily, having stable computational characteristics, and being sensitive to drought (Hong et al. 2015; Hu et al. 2015; Spinoni et al. 2014).

Inner Mongolia grassland in arid and semi-arid regions is one of the most vulnerable areas of the ecological environment, and its response to climate change is also extremely sensitive (Li et al. 2018; Liu et al. 2016; Chen et al. 2013). Climate change has exacerbated the presence of frequent drought and lack of rain in the region, seriously affecting the production and livelihoods of local farmers and herdsmen (Shen et al. 2019). Drought has also restricted economic development in the region. Although there were some previous studies on drought, most of these were limited to using the precipitation data from national meteorological stations, and the accuracy of the results may be affected by the inadequate numbers of stations (Bai et al. 2013; Li et al. 2012, 2014). Meanwhile, the applicability of various drought indices in a semi-arid region needs further discussion. In this work, we attempted to select the proper index which is suitable for drought assessment in the study region from SPI and SPEI, and then analyzed the spatiotemporal distributions of drought characterized by the selected index at different time scales on the basis of the gridded precipitation data set. The results can provide a reference for local water resource management, waterlogging prevention, drought resistance, and ecological protection.

2 Materials and methods

2.1 Study area

We selected the XilinGol League located in the center of the Inner Mongolian Plateau as the study area (115° 13′ ~ 117° 06′ E, 43° 02′ ~ 44° 52′ N). The region has a total area of 200,000 km^2, of which grassland accounts for 95% of the study area. In addition, the study area is also an important part of the agricultural and pasturing interlaced zone of China (Fig. 1). The study area has an arid or semi-arid continental monsoon climate, and the spatial distribution of precipitation is quite varied. In addition, natural disasters such as flooding, drought, frost damage and snowstorms often occur in the study area, especially drought. The local residents suffered a severe drought from 2000 to 2001, when the precipitation and the soil moisture content all fell to record lows, resulting in the reduction of crop yield and the death of a large portion of livestock. Similarly, in mid-June 2018, 193 million m^2 of grassland in nine animal husbandry banners suffered from drought; the number of herdsmen who were affected by the disaster was up to 126,000, and there were 6.51 million affected animals. In this context, the situation regarding the drying up of rivers and the degradation of grassland in the study area is becoming worse.

2.2 Data

We select the gridded daily precipitation data set (with a resolution of 0.5° × 0.5°) from 1962 to 2017 by reason of the

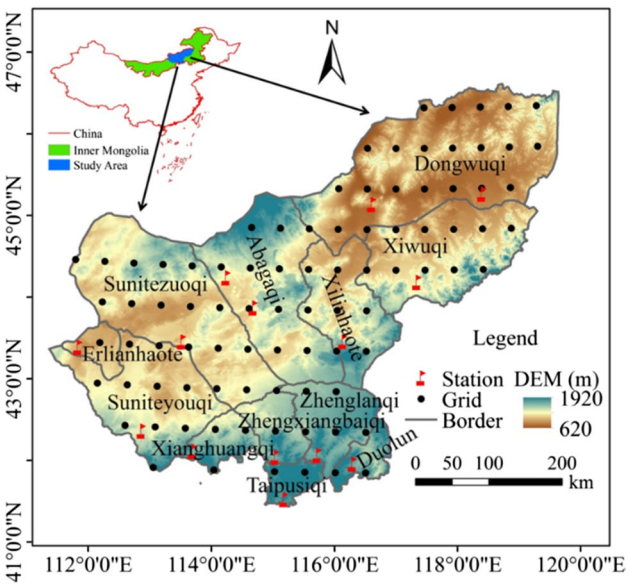

Fig. 1 Distribution of weather stations and 0.5° × 0.5° grid points in study area

few meteorological stations with sufficiently long sequence data in the study area and the lack of coverage of the entire area. This data set came from the National Meteorological Information Center (NMIC) of the China Meteorological Administration (CMA), where it was interpolated by the method of thin plate smoothing spines (TPS) in ANUSPLIN, a software package published by the Australian National University. This analysis can eliminate the influence of elevation and is based on the observed daily precipitation at over 2400 national meteorological stations across China, and the root-mean-square error of this data set is 0.49 mm at a monthly scale. The correlation coefficient between the gridded values and the station values is also as high as 0.93, indicating that the data set has high precision (You et al. 2015; Zhu et al. 2015). On this basis, the SPI was selected to characterize the spatial and temporal distribution of drought in the study area. Meanwhile, we also use the measured daily precipitation data with the same time series from 14 meteorological stations in our study area (Table 1) to validate whether the gridded data were suitable for the study area. Both data sets were provided by the NMIC (http://data.cma.cn).

2.3 Methods

The inverse distance weighted (IDW) method was applied for the gridded data interpolation, this method assumes that each point has a local influence that diminishes with distance, and the value of a point is more affected by near points than by those further away. The spatial correlation of precipitation data accords with this rule, so it is often used in the spatial interpolation of precipitation. Each meteorological station is surrounded by four grid boxes, and the data of each point are most affected by those four grid points. Thus, the nearest four grid boxes around the specific meteorological station are weighted the most in this study (Chen and Liu 2012). What should be noted is that when the station is located at the boundary of the study area, the grids should be extended outside to meet the interpolation requirements. By further comparing the deviation distribution and correlation between the interpolated data and the measured data of the station, we could evaluate whether the precipitation gridded data set was suitable for the analysis of precipitation in the study area. The interpolated date was computed as

$$P_{\mathrm{IDW}} = \frac{\sum_{i=1}^{n} \frac{p_i}{d_i}}{\sum_{i=1}^{n} \frac{1}{d_i}}, \tag{1}$$

where p_i is the precipitation of the neighboring four grid boxes, respectively; d_i is the distance between the station and the four surrounded grids; $n=4$ in this study.

Second, comparing the bias and correlation coefficients between the IDW interpolated data and the observed data from stations (Qiang et al. 2016). The formula of the bias is given as follows:

$$B = \frac{\overline{P_{\mathrm{IDW}}} - \overline{P_{\mathrm{Station}}}}{\overline{P_{\mathrm{Station}}}}, \tag{2}$$

where $\overline{P_{\mathrm{IDW}}}$ is the mean value of interpolated data, and $\overline{P_{\mathrm{Station}}}$ is the means of observed data.

SPI represents the probability of precipitation occurring during a certain period of time. This index can better reflect the intensity and duration of drought at different spatial and temporal scales. In SPI calculations, it is assumed that precipitation variability in a sequence follows a gamma

Table 1 List of the selected meteorological stations in study area

WMO number	Station name	Longitude (°E)	Latitude (°N)	Annual average precipitation (mm)
50,915	Dongwuqi	116.58	45.31	237.53
53068	Erlianhaote	111.58	43.39	125.75
53192	Abagaqi	114.57	44.01	230.20
53195	Suzuoqi	113.38	43.52	173.47
54012	Xiwuqi	117.36	44.35	314.92
54102	Xilinhaote	116.07	43.57	264.53
53083	Narenbaolige	114.09	44.37	210.13
53276	Zhurihe	112.774	42.44	197.60
50913	Wulagai	118.5	45.43	320.91
50924	Huolinguole	119.3	45.32	345.73
53289	Xianghuangqi	113.5	42.14	270.65
54204	Zhengxiangbaiqi	115	42.18	351.22
54205	Zhenglanqi	115.7	42.14	359.61
54305	Taipusiqi	115.16	41.66	383.47

distribution, and after processing the distribution probability of precipitation Γ through normal standardization, a standardized cumulative frequency distribution for precipitation can be applied to classify drought levels (Shi et al. 2017). SPI is computed as (Zhang et al. 2009):

$$g(x) = \frac{1}{\beta^{\alpha}\,\Gamma(\alpha)}\,x^{\alpha-1}\,\mathrm{e}^{-x/\beta}(x>0) \tag{3}$$

$$\Gamma(\alpha) = \int_0^{\infty} y^{\alpha-1}\,\mathrm{e}^{-y}\,\mathrm{d}y, \tag{4}$$

where α and β are shape parameters and scale parameters, respectively; Γ(α) is the gamma function.

The method of maximum likelihood is used to estimate the α and β:

$$\alpha = \frac{1+\sqrt{1+4A/3}}{4A} \tag{5}$$

$$\beta = \frac{\bar{x}}{4A} \tag{6}$$

$$A = \ln(\bar{x}) - \frac{\sum \ln(x)}{n}, \tag{7}$$

where n is the length of the data record, and the cumulative probability of a given time scale can be calculated as follows:

$$G(x) = \int_0^x g(x)\mathrm{d}x = \frac{1}{\beta^{\alpha}\,\Gamma(\alpha)_0}\int_0^x x^{\alpha-1}\,\mathrm{e}^{-\beta}\,\mathrm{d}x. \tag{8}$$

Let $t = x/\beta$, the previous formula can be changed to an incomplete gamma function:

$$G(x) = \frac{1}{\Gamma(\alpha)}\int_0^x x^{\alpha-1}\,e^{-\beta}\,dx \tag{9}$$

$$\alpha = \frac{1+\sqrt{1+4A/3}}{4A},\ \beta = \frac{\bar{x}}{4A} \tag{10}$$

$$A = \ln(\bar{x}) - \frac{\sum \ln(x)}{n}. \tag{11}$$

Since the gamma function does not include the situation of $x = 0$, while the precipitation can be the 0 mm, therefore, the cumulative probability can be expressed as

$$H(x) = q + (1-q)G(x), \tag{12}$$

where the q is the probability when the precipitation is 0. The cumulative probability $H(x)$ can be converted to a standard normal distribution function by the following formula:when $0 \le H(x) \le 0.5$

$$\mathrm{SPI} = -\left(t - \frac{c_0 + c_1 t + c_2 t^2}{1 + d_1 t + d_2 t^2 + d_3 t^3}\right) \tag{13}$$

$$t = \sqrt{\ln\left[\frac{1}{H(x)^2}\right]} \tag{14}$$

when $0.5 < H(x) \le 1$

$$\mathrm{SPI} = -\left(t - \frac{c_0 + c_1 t + c_2 t^2}{1 + d_1 t + d_2 t^2 + d_3 t^3}\right) \tag{15}$$

$$t = \sqrt{\ln\left[\frac{1}{1-H(x)^2}\right]}, \tag{16}$$

where $c_0 = 2.515517$, $c_1 = 0.802853$, $c_2 = 0.010328$, $d_1 = 1.432788$, $d_2 = 0.189269$, $d_3 = 0.001308$.

Similar to SPI, the SPEI is also a kind of multi-scale index for drought, which takes the combined effect of precipitation, temperature and surface evapotranspiration into account. The main steps for calculating SPEI are shown as follows (Vicente et al. 2010a, b).

Monthly potential evapotranspiration (PET) is calculated by the Thornthwaite method (Thornthwaite 1948):

$$\mathrm{PET} = 16K\left(\frac{10T}{I}\right)^{m}, \tag{17}$$

where K is the coefficient of revision based on latitude, T is the monthly mean temperature, I is the annual total heating index, and m is the coefficient determined by I.

Calculation of the water balance, as follows:

$$D_i = P_i - \mathrm{PET}_i, \tag{18}$$

where P_i is the monthly precipitation and PET_i is the monthly potential evapotranspiration.

Fitting the D_i based on three-parameter Log-Logistic distribution and calculating the cumulative function:

$$f(x) = \frac{\beta}{\alpha}\left(\frac{x-y}{\alpha}\right)^{\beta-1}\left[1+\left(\frac{x-y}{\alpha}\right)\right]^{-2} \tag{19}$$

$$F(x) = \left[1+\left(\frac{x-y}{\alpha}\right)^{\beta}\right]^{-1}, \tag{20}$$

where α is the scale parameter, β is the shape parameter, γ is the origin parameter, $f(x)$ is the probability density function, and $F(x)$ is the probability distribution function:

$$\mathrm{SPEI} = W - \frac{C_0 + C_1 + C_2 W^2}{1 + d_1 W + d_2 W^2 + d_3 W^3} \quad (21)$$

$$W = \sqrt{-2\ln(P)}, \quad (22)$$

when $P \le 0.5$, $P = F(x)$, and when $P > 0.5$, $P = 1 - F(x)$. The constants are as follows: $C_0 = 2.515517$, $C_1 = 0.802853$, $C_2 = 0.010328$, $d_1 = 1.432788$, $d_2 = 0.189269$, and $d_3 = 0.001308$.

According to the SPI and SPEI normal distribution curve and standards for drought grades, drought can be divided into the following grades (Table 2).

In this paper, SPI_3 and SPI_{12} were used to denote standardized precipitation indices at seasonal and annual scales, respectively. Based on this, drought characteristics in the study area were described by calculating drought frequency and drought area rate. Drought frequency refers to the proportion of years in which drought of a certain grade occurs, relative to the total number of years at some point during 1962–2017. Drought area rate refers to the proportion of lattice points, where drought of a certain grade occurs, relative to the total number of lattice points. In addition, the scope of influence was divided into the following categories: 0–10% indicates that the drought is not obvious; 10–25% indicates domain drought; 25–33% indicates regional drought; 33–50% indicates partial-local drought, and 50–100% indicates local drought (Xiong et al. 2013).

Table 2 Drought grades classified with SPI and SPEI

Grade	Category	SPI	SPEI
1	No drought	$-0.5 < \mathrm{SPI}$	$-0.5 < \mathrm{SPEI}$
2	Light drought	$-1.0 < \mathrm{SPI} \le -0.5$	$-1.0 < \mathrm{SPEI} \le -0.5$
3	Moderate drought	$-1.5 < \mathrm{SPI} \le -1.0$	$-1.5 < \mathrm{SPEI} \le -1.0$
4	Severe drought	$-2.0 < \mathrm{SPI} \le -1.5$	$-2.0 < \mathrm{SPEI} \le -1.5$
5	Extreme drought	$\mathrm{SPI} \le -2.0$	$\mathrm{SPEI} \le -2.0$

3 Results

3.1 Precipitation change background

There were 88 grid points in the study area (Fig. 1). In comparing the deviation distribution and correlation between the IDW interpolated data and the measured data of the stations, the bias of precipitation at the Erlianhaote station was 17.33%, while the absolute values of other stations were all less than 15% (Fig. 2a). The vast majority were less than 10%, accounting for 71.43% of the total number of stations. In addition, there was a very good linear relationship between the station data and the interpolated data ($R^2 = 0.98$; $P < 0.0001$). Furthermore, the slope of the fitted linear equation was 1.08, which is close to 1.00 (Fig. 2b). Therefore, the gridded data set can reflect the spatiotemporal patterns of precipitation distributions in the study area, and it can also replace the measured station precipitation data to calculate the drought indexes.

The spatial pattern of the annual precipitation in the study area from 1962 to 2017 exhibits the obvious feature of "high in the east and low in the west", with a gradual decline from 408.14 mm in the eastern region to 137.26 mm in the western region. The difference between the annual precipitation in the eastern and western areas is as high as 270 mm (Fig. 3a). Moreover, the precipitation in the northeast region exhibits an upward trend with a velocity in excess of 3 mm per decade (mm decade^{-1}), but the region with an increasing trend of precipitation only accounts for 43.2% of the total area. The remaining 56.8% of the area has an insignificant decreasing trend, mainly being located in the central part of the study area (Fig. 3b).

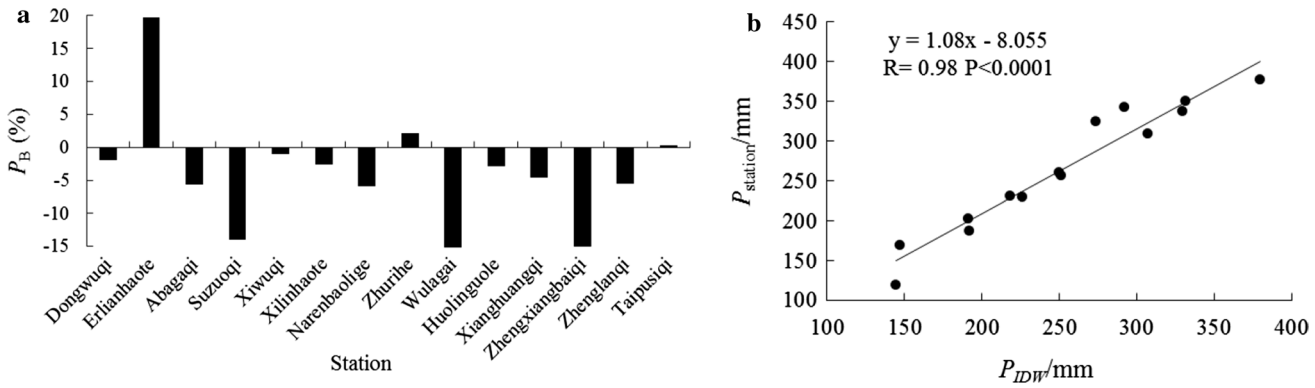

Fig. 2 Relationship between annual average precipitation and interpolated grids of the study area (the two data sets have a good linear relationship, $R^2 = 0.98$, $P < 0.0001$, and the slope of the fitted linear equation was 1.08)

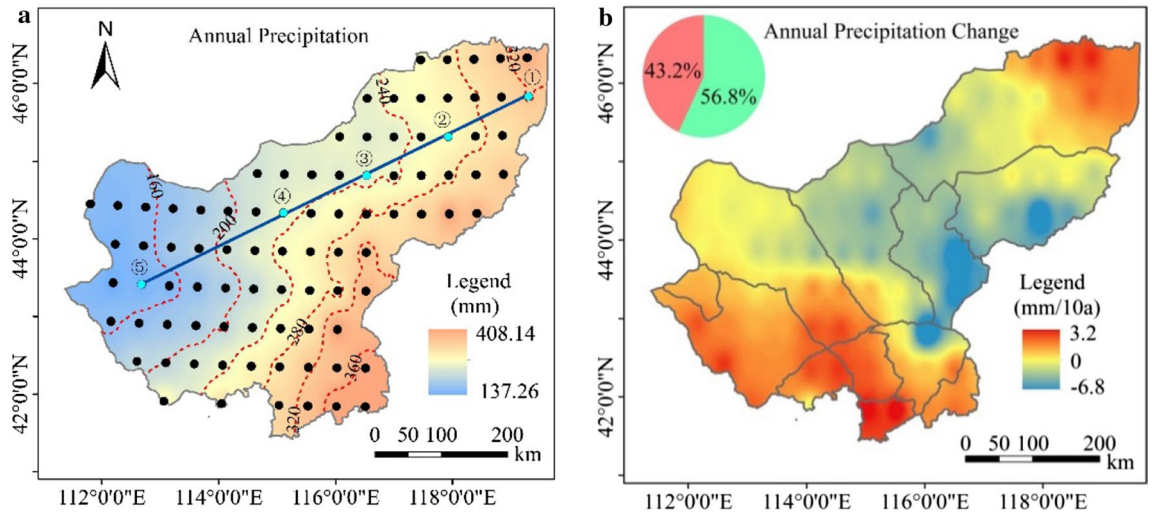

Fig. 3 Spatiotemporal distribution of the annual precipitation of the study area. (The red part of the pie chart represents the proportion of the increasing trend, which accounts for 43.2% of the total area, while the green represents the proportion of the decreasing trend, accounts for 56.8% of the total area)

3.2 Applicability of drought index

Before analyzing the spatiotemporal characteristics of drought in the study area, we should select the drought index suitable for the region first. According to the spatial distribution of precipitation, we picked five grid points (Fig. 3a) to calculate their SPI and SPEI at annual scale, and compared the spatiotemporal distribution results presented by the two indices with historical drought records in the study area, the annual variations are shown in Fig. 4. In general, although the variation trends of SPEI and SPI at annual scale are basically the same, there is a big difference in the recognition of drought degree. In terms of the grid point ①, the drought year detected by SPEI and SPI were 14 years and 17 years, respectively. In addition, in years when were identified as the drought by both indices, the degree of drought detected by SPI is generally more severe than that detected by SPEI. It can be seen from Fig. 4b that the severe drought years identified by SPI were 5 years, which were 1997, 1999, 2006, 2008, and 2017. However, the results of SPEI showed that there was no severe drought year experienced throughout the study period. Similarly, SPI shows that there have been six severe drought years at grid point ④, most of which occurred after the late 1990s, and SPEI also did not detect the severe drought year (Fig. 4d). Although the grid point ③ had fewer drought events during the study period, the degree of drought detected by SPI at this point was also more severe than SPEI (Fig. 4c).For grid point ⑤, the annual precipitation of which is the least among the five grid points, there were three extreme drought events occurred in 1980, 2001, and 2005, while SPEI did not detect the extreme drought events during this period (Fig. 4e).

Furthermore, we selected three typical drought years recorded in history to verify the spatial distribution of drought presented by SPI and SPEI. As can be seen from Fig. 5a_1, the SPI showed that the areas where light drought occurred in the study area were mainly in the central and western regions, and the moderate or even severe drought experienced in the northeast in 1962. However, the SPEI indicated that only the light drought occurred in almost the whole study area in 1962 (Fig. 5a_2). In 1965, the areas where severe drought and extreme drought were detected by SPI were located in the middle and south of the study area (Fig. 5b_1). While the SPEI did not detect the extreme drought events, only the severe drought events were detected in a small area in the south (Fig. 5b_2). From Fig. 5c_2, we can find that the area of severe and extreme drought detected by SPI account for more than a half of the study area in 1980 (Fig. 5c_1), while SPEI showed that there were only light and moderate drought occurred in the study area (Fig. 5c_2).

Overall, the drought situations described by SPI were much more consistent with the historical drought records in our study area. Therefore, we select SPI as the indicator of this work for further discussion.

3.3 Spatiotemporal variations of drought at annual scale

By calculating the SPI of 88 grid points and further identifying the corresponding degree of drought events in the study area, the frequency and variability of various drought events in different periods were obtained, as shown in Fig. 6. The frequency of light drought in the study area was the

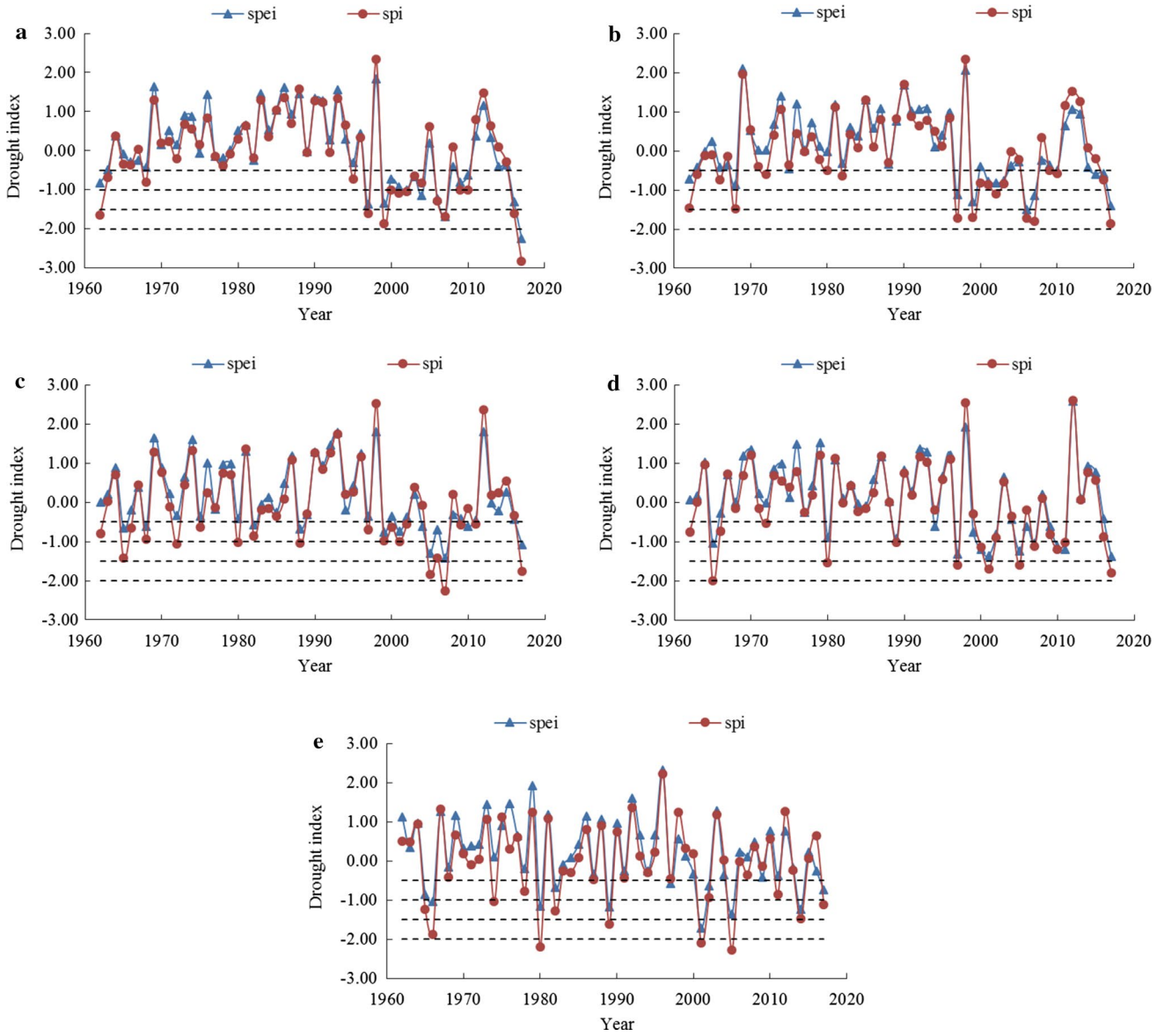

Fig. 4 Annual variations of SPI and SPEI in the study area for period 1962–2017. **a** Grid point ①, **b** grid point ②, **c** grid point ③, **d** grid point ④, **e** grid point ⑤

highest across the different periods, followed by moderate, severe, and extreme drought. The occurrence of light drought in the study area declined during the last 56 years. During this time, the frequency of light drought was lowest in the 1980s, and its frequency increased to some extent during the next 20 years. However, the frequency of light drought sharply decreased after 2010. During the research sequence, the frequency of moderate drought increased, with 133 drought events in 2001–2010. Meanwhile, the frequency of severe drought was also on the rise, and the highest frequency was also reached between 2001 and 2010. As for the extreme drought, the frequency was also on the rise. However, no extreme drought events were detected between 1981 and 1990. After that, the frequency of extreme droughts increased sharply and reached its highest level between 2001 and 2010. Overall, the frequency of light drought in the study area has decreased, but the frequency of the other three types of drought events has increased, and the frequency of various types of drought events reached the highest level in the period 2001–2010.

We analyzed the SPI of each grid point for nearly the entire 56 years. The spatial distribution of different drought degrees in the study area is shown in Fig. 7. All of the regions of the study area experienced light drought events, with the drought rate ranging from 3.58 to 26.76%. The drought rate for the central region was lower, while the

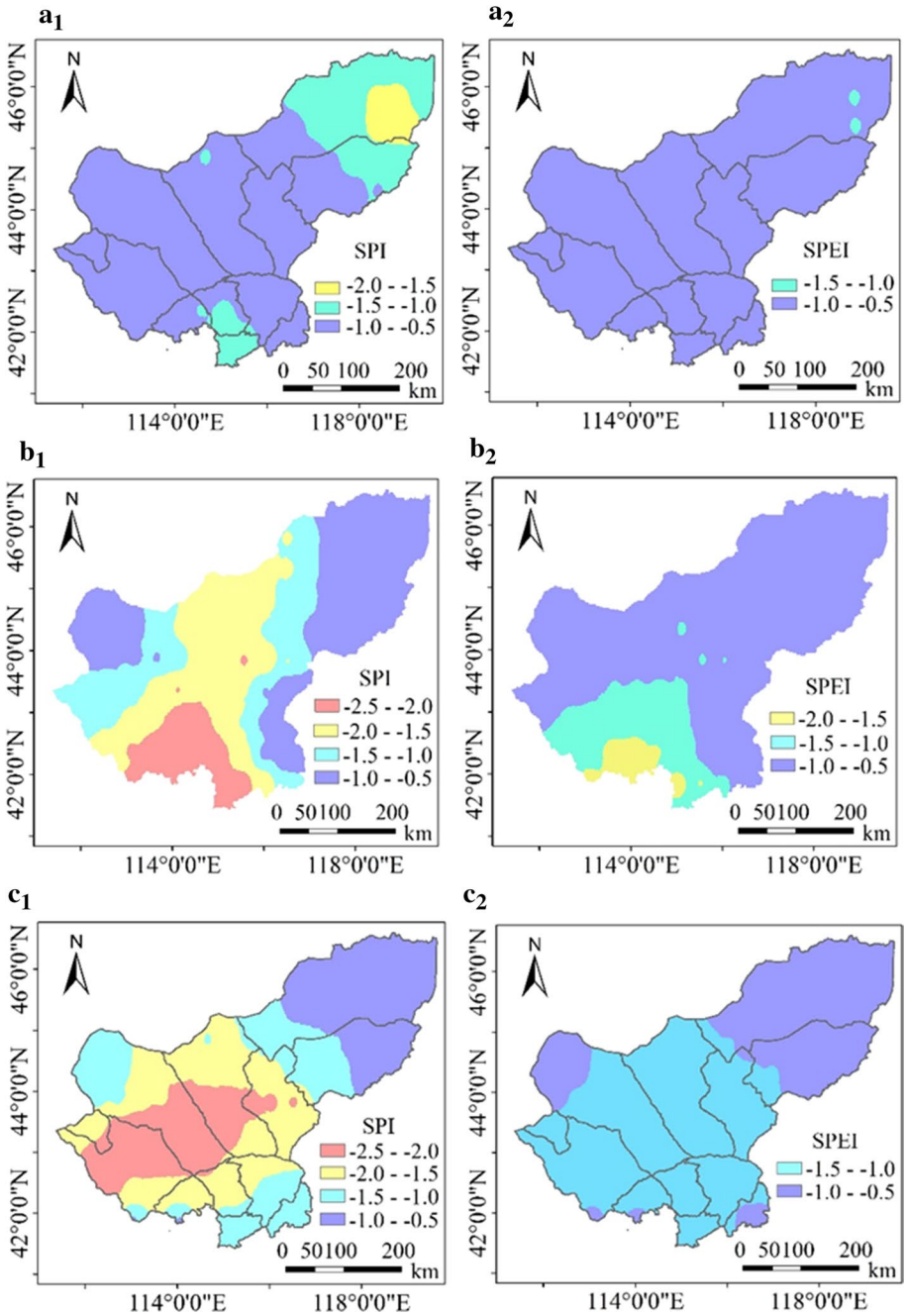

Fig. 5 Spatial distribution of SPI and SPEI in 1962, 1965 and 1980. $\mathbf{a}_1$ SPI in 1962, $\mathbf{a}_2$ SPEI in 1962, $\mathbf{b}_1$ SPI in 1965, $\mathbf{b}_2$ SPEI in 1965, $\mathbf{c}_1$ SPI in 1980, $\mathbf{c}_2$ SPEI in 1980

incidence of light drought for the south-central and southern regions were relatively higher. Likewise, the moderate drought events also covered the whole study area, with the rates in the range of 1.79–16.06% (Fig. 7b).

The spatial distribution of the high-frequency and low-frequency regions in moderate drought was not concentrated, while the south-central region was the high-risk area for moderate drought. Similarly, the south-central region was also a high-frequency area for severe drought, with the highest drought rate of 12.50%. Meanwhile, the central and eastern regions also experienced severe drought events, but not over the entire area (Fig. 7c). From Fig. 7d, we can see that the maximum frequency of the extreme drought in the study area was 7.14%, mainly concentrated in the western, south-central, and northeastern regions, while no extreme drought events occurred in the northern region.

From the perspective of the overall spatial distribution the frequency of light drought, moderate drought, severe drought, and extreme drought in the study area decreased grade by grade, making it more common for each region to experience light drought, and with fewer regions experiencing extreme drought. In addition, the frequency of various

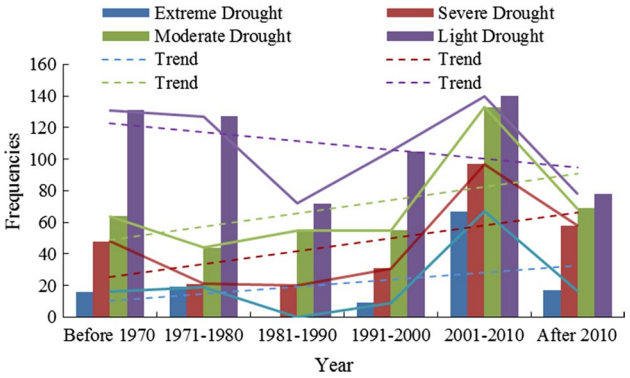

Fig. 6 Frequency of annual drought events in the study area for period 1962–2017

drought events in the north-central region of the study area was lower, while the central and southern regions are areas, where various drought events occurred frequently.

3.4 Spatiotemporal variations of Drought at Seasonal Scale

Trends of different drought events based on the SPI at the seasonal scale are shown in Fig. 8. The frequency of the extreme drought in spring showed an upward trend, and the frequency of the other three categories of droughts tended to decline. There were no extreme drought events before 1970 or during the 1980s, while after 2010, the frequency of extreme drought in spring reached 89, which was higher than that of light drought during the same period. Aside from this, the frequency of light drought in other periods was always the highest (Fig. 8a). In summer, the frequency of various drought events was on the rise; as can be also seen from Fig. 8b, the frequency of moderate drought in the study area was the highest, reaching 162 between 2001 and 2010, followed in decreasing order by light, extreme and severe drought. Meanwhile, the frequency of each kind of drought event during this period was higher than that of the same kind of event during the rest of the period. As a result, the study area was affected by drought most severely during the summers of 2001–2010.

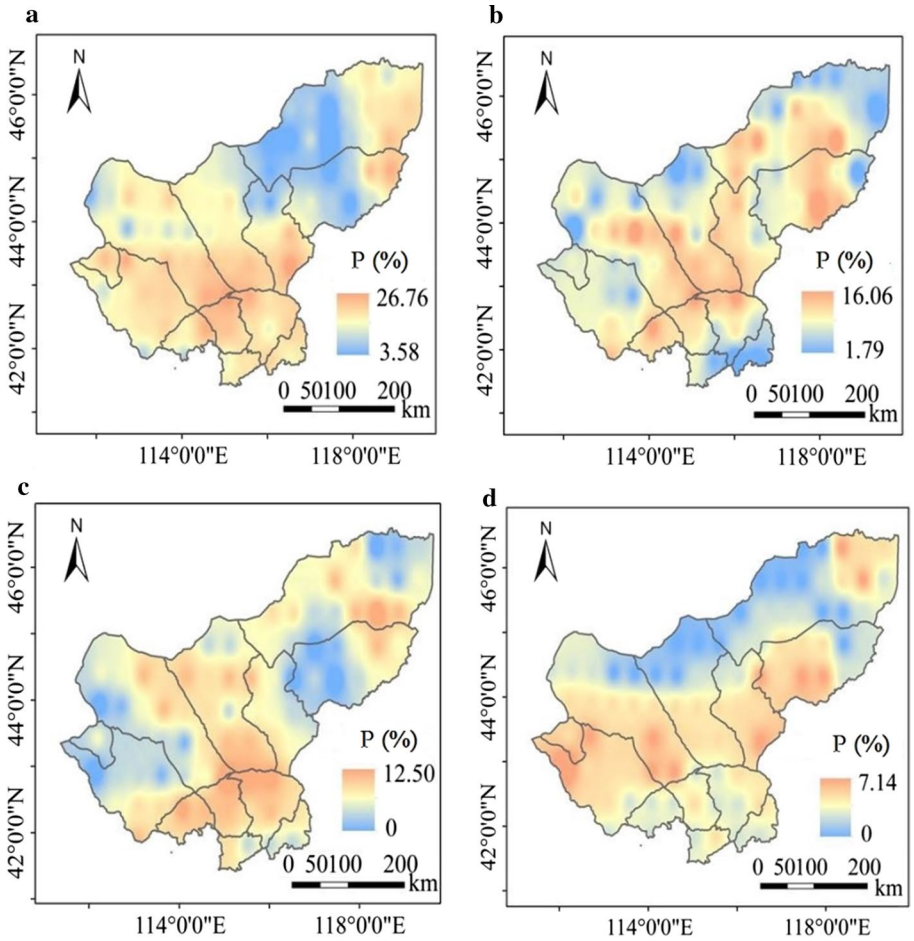

Fig. 7 Spatiotemporal distribution of the annual drought events. **a** Light drought, **b** moderate drought, **c** severe drought, **d** extreme drought

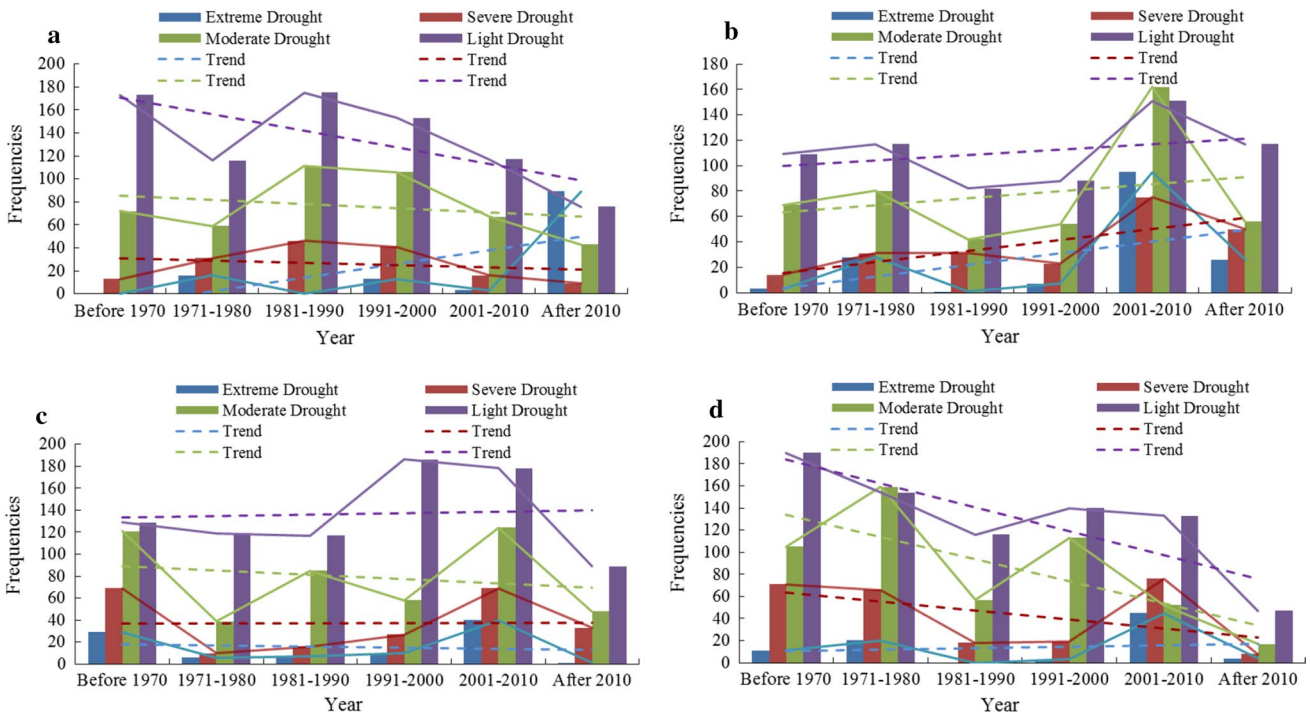

Fig. 8 Frequency of seasonal drought events in the study area for period 1962–2017. **a** Spring, **b** Summer, **c** Autumn, **d** Winter

In addition to the declining trend of the moderate drought in autumn, the other three types of drought showed a slight upward trend, and the frequencies of the four types of drought events in each period followed the pattern light drought, moderate drought, severe drought and extreme drought in decreasing order (Fig. 8c). In winter, the extreme drought frequency rose slightly, while other kinds of drought declined. In the 1970s, the frequencies of moderate drought were the highest at 159, and the frequency of severe drought was 76 during 2001–2010, exceeding that of moderate drought during the same period. By comparing the average frequency of various drought events in different seasons, it was observed that light drought occurred more frequently in autumn, with the highest average frequency of 136. The moderate and severe drought events occurred more frequently in winter, with their highest average frequencies of 84 and 43, respectively, while the extreme drought events occurred more frequently in summer, with the highest frequency of 27.

In terms of the spatial distribution of drought in different seasons, the spring light drought occurred more frequently in the central and western parts of the study area, with the highest rate of 28.57% in the western region, and the probability in the northeast region was lower (Fig. 9a_1). The probability of the moderate drought in spring was between 3.57 and 17.86% and occurred more frequently in the central and southwest regions (Fig. 9a_2). The severe drought in spring occurred mostly in the southern part of the study area, while the severe drought was not detected in the western region (Fig. 9a_3). In spring, the extreme drought events covered the entire study area, but the probability of an event was lower, especially in the central and western regions, where the probability was 1.79%. Meanwhile, extreme drought occurred more frequently in the northeast, with a probability of 7.14% (Fig. 9a_4).

In summer, both the light and moderate drought events occurred, but with different spatial distributions. The light drought was concentrated in the north and northeastern regions with the highest occurrence probability of 23.20%, while moderate drought was mainly concentrated in the central region of the study area, with the highest frequency of 16.06%, and the probability in the low-frequency region was only 1.80% (Fig. 9b_1, b_2). In contrast to the above patterns, the severe and extreme drought both occurred only in local areas within the Xilingol League territory. For example, the severe drought often occurred in the western and southern regions, while the extreme drought mainly occurred in the central and northeastern parts of the study area, with the highest probabilities of 10.71% and 7.14%, respectively (Fig. 9b_3, b_4).

The frequency of the light drought in autumn was between 3.61 and 28.55%, and the locations where it occurred more frequently were mainly in the central and southern regions, similar to the spatial distribution of light drought. The locations where the moderate drought occurred with high frequency were also in the central and southern

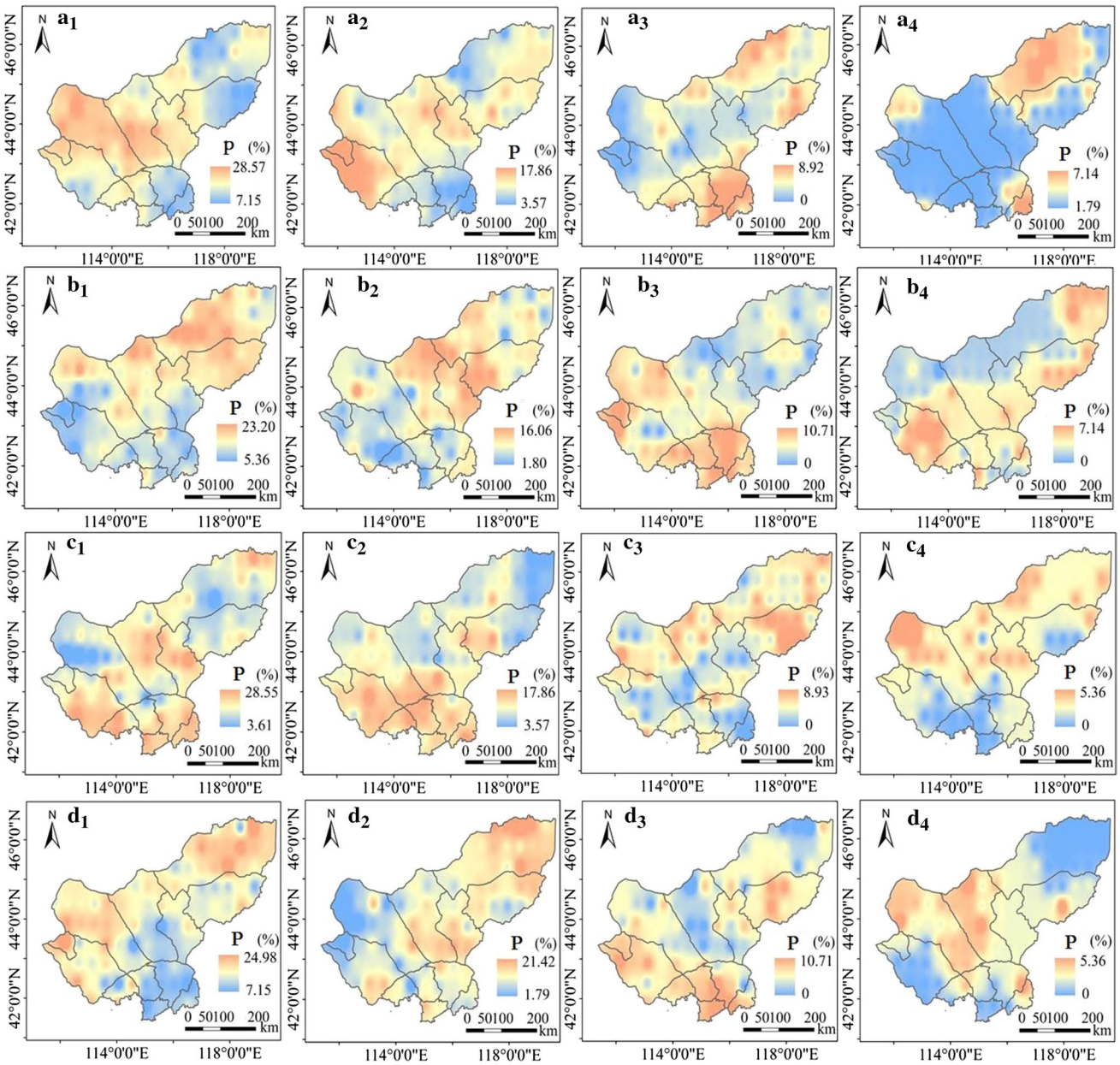

Fig. 9 Spatiotemporal distribution of seasonal drought events. **a** Spring, **b** Summer, **c** Autumn, **d** Winter, 1: Light drought, 2: Moderate drought, 3: Severe drought, 4: Extreme drought)

regions, but the probability declined to some extent, ranging from 3.57 to 17.86%. We can also see that neither the severe drought nor the extreme drought covered the entire study area; the spatial distribution of the extreme drought was relatively concentrated, and the locations where it occurred with high frequency were in the north and northeastern parts (Fig. 9c). It can be seen from Fig. 9d that the drought in this area often occurred in winter; the frequencies of moderate drought and severe drought were the highest across the four seasons in the northeast and south of the study area, while the extreme drought in winter is mainly concentrated in the middle of the study area, with the highest probability of 5.36%.

The variation in the station frequency ratio for different categories of drought events at a seasonal scale is shown in Fig. 10. The domain drought was relatively common across all seasons in the study sequence, and the partial-local light drought usually occurred in spring; moreover, the local light drought occurred in the spring of 1984 (Fig. 10a). In summer, no local light drought occurred during a period of 19 years. In summer, not only did the domain light drought occur in 19 years, but regional light drought occurred in

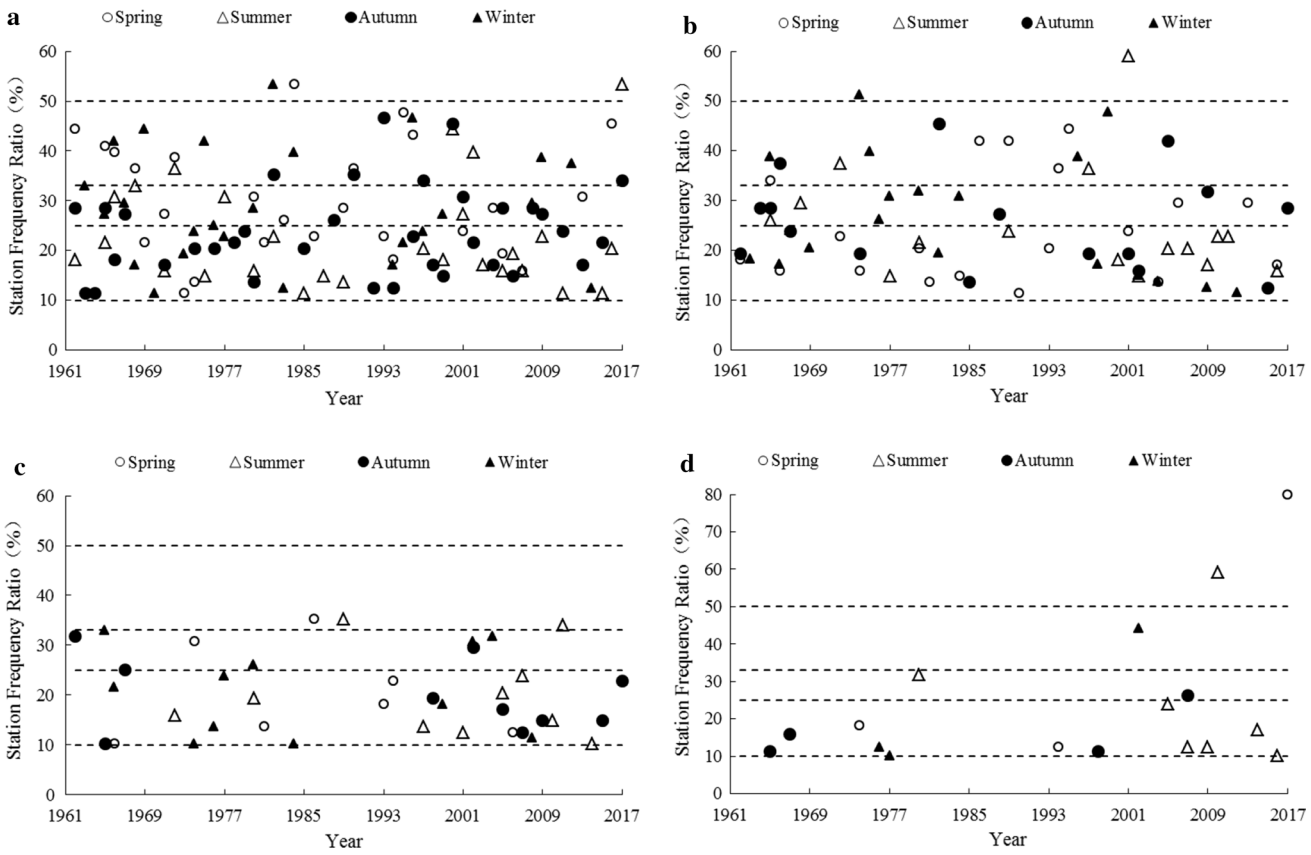

Fig. 10 Station frequency ratio of seasonal drought events in the study area for period 1962–2017. **a** Light drought, **b** moderate drought, **c** severe drought, **d** extreme drought

4 years, and the partial-local light drought occurred in 3 years. In addition, there was a local light drought in the summer of 2017. The domain light drought in autumn and winter occurred throughout most of the study period, and a local light drought occurred in the winter of 1982. On the whole, large-scale light drought occurred in a more concentrated manner across all seasons in the 1990s. In terms of the moderate drought (Fig. 10b), the local moderate drought occurred in the summer and winter of 2001 and 1974, respectively. At the same time, the partial-local moderate drought occurred in the summers of 1972 and 1997, and there were five, three, and four respective years when the partial-local moderate drought occurred in spring, autumn, and winter. In addition, there were 4 years when the regional moderate drought occurred in winter in the mid-1970s to the mid-1980s. During the whole study period, the domain moderate drought occurred in 10 years in summer and winter, and most of these occurred after 2000. Figure 10c shows that large-scale severe drought events occurred in all seasons after 1993, but there was no local severe drought. Only in spring and summer in 1986, 1989, and 2011 did the partial-local severe drought occur. There were 7 years with extreme drought events in summer, including a local extreme drought in 2010, and domain extreme drought occurred in 2005, 2007, 2009, 2014, and 2016. In winter, the partial-local extreme drought occurred only in 2002, and the domain extreme drought occurred only in spring in 1974 and 1994 (Fig. 10d).

4 Discussion

Xilingol League is located in the Inner Mongolian Plateau and is surrounded by the Great Khingan and Yinshan Mountains. It is difficult for warm and moist airflow to enter this region, resulting in the climatic characteristics of strong evaporation and insufficient precipitation (Zhou et al. 2013). During the past 56 years, drought events in the study area have been dominated by light and moderate drought with increasing frequency, which is consistent with the findings of most researchers (Bai et al. 2013; Zhou et al. 2013). Some studies have shown that in recent decades, rising atmospheric pressure caused by abnormal circulation at high latitudes and the reduction of the northward transport of water vapor caused by weakening of the East Asian Monsoon are among the causes of severe drought in

northern China (Huang et al. 2015). However, the East Asian Monsoon has strengthened with time, resulting in a slight alleviation of drought during each season for the study area (Cheng et al. 2013). Land utilization and land cover change caused by the transformation of the underlying surface of the watershed have also had important effects on climate change (Li et al. 2010), which may lead to the agricultural drought (Shen et al. 2019), as we know, there is a transmission relation between the meteorological drought and the agricultural drought, the further research focus on the relationship between the two categories of drought will be very interesting.

The Standardized Precipitation Index selected in this paper also only includes precipitation as a factor, but the factors that lead to drought are more complicated. Therefore, future research will comprehensively consider hydrometeorological factors to clarify the evolution of drought and then improve prediction and early warning measures.

5 Conclusions

Based on the gridded precipitation data set with a horizontal resolution of 0.5° × 0.5° of Xilingol League from 1962 to 2017, we compared the applicability of SPI and SPEI for drought assessment in the study area, and selected the proper index to analyze the spatial and temporal distribution of drought at different time scales during the past 56 years. The results reflect the drought evolution of the study area. The main conclusions follow.

(1) The gridded precipitation data set is suitable for the characterization of drought distribution in the study area, and the spatial pattern of precipitation is obviously characterized by the "high in east and low in west" rule. Meanwhile, a non-significantly decreasing inter-annual tendency was found during the 56 years, mainly in the center of the study area. The drought conditions described by SPI were much more consistent with the historical drought records in our study area.

(2) The frequency of light, moderate, severe and extreme drought events in the study area decreased grade by grade, and the drought events occurred more frequently in the south-central region. During the past 56 years, the frequency of light drought in the study area has decreased, while the frequencies of the moderate, severe and extreme droughts have all increased to some extent, indicating that the drought degree in the study area has increased.

(3) The light drought occurred mostly in the autumn and was mainly distributed in the central and southern parts of the study area. The moderate drought and severe drought occurred mostly in the winter and were concentrated in the northeast and south of the study area, while the extreme drought events often occurred in the summer, and the highest frequency area was in the western part of the study region. In addition, the frequencies of different degrees of drought in summer showed an upward trend. The study area was most severely affected by the drought during 2001–2010.

(4) A wide range of light drought events occurred in the study area in the 1990s. Among these, the spring, summer and winter experienced local drought in 1984, 2017, and 1982, respectively. In the summer and winter seasons, local moderate drought occurred in 2001 and 1974, and the domain moderate drought in these two seasons mainly occurred after 2000. Large-scale severe drought events occurred in all seasons in a more concentrated manner after 1993, and there was a local extreme drought in the summer of 2010.

Acknowledgements This work was financially supported by the Fundamental Research Fund of the China Institute of Water Resources and Hydropower Research (Grant MK2019J09, MK2016J27); the Natural Science Foundation of Inner Mongolia Autonomous Region of China (Grant 2017BS0512); the National Key R&D Program of China (Grant 2018YFC0406400); the Science and technology plan key project of Inner Mongolia Autonomous Region of China (2018); the National Natural Science Foundation of China (Grant 51620105003, 51869017, 51479086, 51369016); the program for Young Talents of Science and Technology in Universities of Inner Mongolia Autonomous Region (Grant NJYT-18-B11); the Ministry of Education Innovative Research Team (Grant IRT_17R60); the Ministry of Science and Technology Innovative Research Team in Priority Areas (Grant 2015RA4013).

References

Bai ML, Li JT, Li XC et al (2013) Spring and summer drought characteristics in central and eastern inner mongolia nearly 50 years. J Arid Land Resour Environ 27:131–136. https://doi.org/10.13448/j.cnki.jalre.2013.05.028

Chen FW, Liu CW (2012) Estimation of the spatial rainfall distribution using inverse distance weighting (IDW) in the middle of Taiwan. Paddy Water Environ 10:209–222. https://doi.org/10.1007/s10333-012-0319-1

Chen LP, Zhao NX, Zhang LH et al (2013) Responses of two dominant plant species to drought stress and defoliation in the Inner Mongolia Steppe of China. Plant Ecol 214:221–229. https://doi.org/10.1007/s11258-012-0161-y

Cheng L, Liu HW, Zhou TJ et al (2013) Inter-decadal variations of summer southeast and southwest monsoon frequency over East Asia and its relationship with snow cover over the Tibetan Plateau for recent 30 years. Chin J Atmos Sci 37:1326–1336. https://doi.org/10.3878/j.issn.1006-9895.2013.12189

Dai AG (2011) Drought under global warming: a review. Wiley Interdiscip Rev Clim Change 2:45–65. https://doi.org/10.1002/wcc.81

Dai AG, Trenberth KE, Qian TT (2004) A global dataset of palmer drought severity index for 1870–2002: relationship with soil moisture and effects of surface warming. J Hydrometeor 5:1117–1130. https://doi.org/10.1175/JHM-386.1

Hong XJ, Guo SL, Xiong LH et al (2015) Spatial and temporal analysis of drought using entropy-based Standardized Precipitation Index: a case study in Poyang Lake basin, China. Theor Appl Climatol 122:543–556. https://doi.org/10.1007/s00704-014-1312-y

Hu Q, Pan FF, Pan XB et al (2015) Spatial analysis of climate change in Inner Mongolia during 1961–2012, China. Appl Geogr 60:254–260. https://doi.org/10.1016/j.apgeog.2014.10.009

Huang J, Sun SL, Xue Y et al (2015) Changing characteristics of precipitation during 1960–2012 in Inner Mongolia, northern China. Meteorol Atmos Phys 127:257–271. https://doi.org/10.1007/s00703-014-0363-z

IPCC (2013) Summary for policy makers of the synthesis report of the IPCC fifth assessment report. Cambridge University Press, Cambridge

Li XL, Zhang CJ, Yang QL et al (2010) Climatic variations and human activities in Lujiagou, Dingxi Region over the past 11200 years. J Arid Land Resour Environ 24:88–93. https://doi.org/10.13448/j.cnki.jalre.2010.11.008

Li SY, Verburg PH, Lv SH et al (2012) Spatial analysis of the driving factors of grassland degradation under conditions of climate change and intensive use in Inner Mongolia, China. Reg Environ Change 12:461–474. https://doi.org/10.1007/s10113-011-0264-3

Li R, Tsunekawa A, Tsubo M (2014) Index-based assessment of agricultural drought in a semi-arid region of Inner Mongolia. China. J. Arid Land 6:3–15. https://doi.org/10.1007/s40333-013-0193-8

Li W, Duan LM, Luo YY et al (2018) Spatiotemporal characteristics of extreme precipitation regimes in the Eastern Inland river basin of Inner Mongolian Plateau, China. Water 10:35. https://doi.org/10.3390/w10010035

Liu SL, Kang WP, Wang T (2016) Drought variability in Inner Mongolia of northern China during 1960–2013 based on Standardized Precipitation Evapotranspiration Index. Environ Earth Sci 75:145. https://doi.org/10.1007/s12665-015-4996-0

Patel NR, Chopra P, Dadhwal VK (2007) Analyzing spatial patterns of meteorological drought using Standardized Precipitation Index. Meteorol Appl 14:329–336. https://doi.org/10.1002/met.33

Qiang F, Zhang MJ, Wang SJ et al (2016) Estimation of areal precipitation in the Qilian Mountains based on a gridded dataset since 1961. J Geogr Sci 26:59–69. https://doi.org/10.1007/s11442-016-1254-7

Shen ZX, Zhang Q, Singh VP et al (2019) Agricultural drought monitoring across Inner Mongolia, China: model development, spatiotemporal patterns and impacts. J Hydrol 571:793–804. https://doi.org/10.1016/j.jhydrol.2019.02.028

Shi BL, Zhu XY, Hu YC et al (2017) Drought characteristics of Henan province in 1961-2013 based on Standardized Precipitation Evapotranspiration Index. J Geogr Sci 27:311–325. https://doi.org/10.1007/s11442-017-1378-4

Spinoni J, Naumann G, Carrao H et al (2014) World drought frequency, duration, and severity for 1951–2010. Int J Climatol 34:2792–2804. https://doi.org/10.1002/joc.3875

Tao H, Borth H, Fraedrich K et al (2014) Drought and wetness variability in the river basin and connection to large-scale atmospheric circulation. Int J Climatol 34:2678–2684. https://doi.org/10.1002/joc.3867

Thornthwaite CW (1948) An approach toward a rational classification of climate. Geogr Rev 38(1):55–94. https://doi.org/10.2307/210739

Vicente SM, Beguería S, López JI (2010a) A multiscalar drought index sensitive to global warming: the Standardized Precipitation Evapotranspiration Index. J Clim 23(7):1696–1718. https://doi.org/10.1175/2009JCLI2909.1

Vicente SM, Beguería S, López JI et al (2010b) A new global 0.5° gridded dataset (1901–2006)of a multiscalar drought index: comparison with current drought index datasets based on the palmer drought severity index. J Hydrometeorol 11:1033–1043. https://doi.org/10.1175/2010JHM1224.1

Wang QF, Wu JJ, Lei TJ et al (2014) Temporal-spatial characteristics of severe drought events and their impact on agriculture on a global scale. Quatern Int 349:10–21. https://doi.org/10.1016/j.quaint.2014.06.021

Wang YM, Ren FM, Zhao YL et al (2017) Comparison of two drought indices in studying regional meteorological drought events in China. J Meteorol Res 31:187–195. https://doi.org/10.1007/s13351-017-6075-9

Wen KG, Shen JG (2006) China meteorological disaster code: inner mongolia volume. China Meteorological Press, Beijing

Woodhouse CA, Overpeck JT (1998) 2000 years of drought variability in the central United States. Bull Am Meteorol Soc 79:2693–2714. https://doi.org/10.1175/1520-0477(1998)079%3c2693:YODVIT%3e2.0.CO;2

Wu H, Svoboda MD, Hayes MJ et al (2007) Appropriate application of the Standardized Precipitation Index in arid locations and dry seasons. Int J Climatol 27:65–79. https://doi.org/10.1002/joc.1371

Xiong GJ, Zhang BK, Li CY et al (2013) Characteristics of drought variations in Southwest China in 1961–2012 based on SPEI. Climate Change Research 9(3):192–198. https://doi.org/10.3969/j.issn.1673-1719.2013.03.006

You QL, Zhang MJ, Zhang W et al (2015) Comparison of multiple datasets with gridded precipitation observations over the Tibetan Plateau. Clim Dyn 45:791–806. https://doi.org/10.1007/s00382-014-2310-6

Yu MX, Li QF, Hayes MJ et al (2014a) Are droughts becoming more frequent or severe in China based on the Standardized Precipitation Evapotranspiration Index: 1951–2010? Int J Climatol 34:545–558. https://doi.org/10.1002/joc.3701

Yu XY, He XY, Zheng HF et al (2014b) Spatial and temporal analysis of drought risk during the crop-growing season over northeast China. Nat Hazards 71:275–289. https://doi.org/10.1007/s11069-013-0909-2

Zhang Q, Xu CY, Zhang ZX (2009) Observed changes of drought/wetness episodes in the Pearl River basin, China, using the Standardized Precipitation Index and aridity index. Theor Appl Climatol 98:89–99. https://doi.org/10.1007/s00704-008-0095-4

Zhang MJ, He JU, Wang BL et al (2013) Extreme drought changes in Southwest China from 1960 to 2009. J Geogr Sci 23:3–16. https://doi.org/10.1007/s11442-013-0989-7

Zhou Y, Li N, Ji ZH (2013) Temporal and spatial patterns of droughts based on Standard Precipitation Index (SPI) in Inner Mongolia during 1981–2010. J Nat Res 28(10):1694–1706. https://doi.org/10.11849/zrzyxb.2013.10.005

Zhu XF, Zhang MJ, Wang SJ et al (2015) Comparison of monthly precipitation derived from high-resolution gridded datasets in arid Xinjiang, central Asia. Quatern Int 358:160–170. https://doi.org/10.1016/j.quaint.2014.12.027

Zuo DD, Feng GL, Zhang ZP et al (2018) Application of Archimedean Copulas to the analysis of drought decadal variation in China. Asia Pac J Atmos Sci 54:125–143. https://doi.org/10.1007/s13143-017-0065-9